Title: Multi-approach analysis to assess the chromium(III) immobilization by *Ochrobactrum anthropi* DE2010

Abstract

Ochrobactrum anthropi DE2010 is a microorganism isolated from Ebro Delta microbial mats and able to resist high doses of chromium(III) due to its capacity to tolerate, absorb and accumulate this metal. The effect of this pollutant on *O. anthropi* DE2010 has been studied assessing changes in viability and biomass, sorption yields and removal efficiencies. Furthermore, and for the first time, its capacity for immobilizing Cr(III) from culture media was tested by a combination of High Angle Annular Dark Field (HAADF) Scanning Transmission Electron Microscopy (STEM) imaging coupled to Energy Dispersive X-ray spectroscopy (EDX).

The results showed that *O. anthropi* DE2010 was grown optimally at 0-2 mM Cr(III). On the other hand, from 2 to 10 mM Cr(III) microbial plate counts, growth rates, cell viability, and biomass decreased while extracellular polymeric substances (EPS) production increases. Furthermore, this bacterium had a great ability to remove Cr(III) at 10 mM (q= 950.00 mg g^{-1}) immobilizing it mostly in bright polyphosphate inclusions and secondarily on the cellular surface at the EPS level. Based on these results, *O. anthropi* DE2010 could be considered as a potential agent for bioremediation in Cr(III) contaminated environments.

Keywords: Ochrobactrum anthropi DE2010; CLSM; ICP-OES; HAADF-STEM EDX; polyphosphate inclusions

1. Introduction

The increase in industrial and anthropogenic activities has largely contributed towards the introduction of heavy metals and other pollutants into the environment (Gupta et al., 2014; Bhattacharya et al., 2015). Pollution by heavy metals has become a serious threat to the environment and public health, since, in general, they are highly toxic and accumulate throughout the food chain (Feng et al., 2012; Xu et al., 2014).

Chromium is one of the earth crust's most abundant elements (Mohana and Pittman, 2006) and it is a redox active 3d transition metal with different oxidation states ranging from 2+ to 6+ (Greenwood and Earnshaw, 1998; Srivastava and Thakur, 2007). The trivalent (Cr(III)) and hexavalent (Cr(VI)) forms, from industrial by-products or by being part of phosphate fertilizers used in agriculture (Nziguheba and Smolders, 2008; Manahan, 2009) among other chromium sources, are stable in the majority of terrestrial surface and aquatic environments (Kimbrough et al., 1999; Ihsanullah et al., 2016). Cr(III) is considered to be an essential element (micronutrient) with known cellular biological functions (Balk et al., 2007; Evert et al., 2013). However, with long-term exposure it can produce toxic effects in the cells, but at a much lower degree than Cr(VI), which is more toxic and unhealthy for living beings and the environment (Shanker et al., 2005; Francisco et al., 2011; Ihsanullah et al., 2016). Even so, Cr(III) is involved in some human diseases such as: structural perturbation in erythrocyte membrane and cancer (Kusiak et al., 1993; Suwalsky et al., 2008; Figgit et al., 2010).

In the last decade, our research group has isolated different heterotrophic and phototrophic (cyanobacteria and algae) microorganisms from the Ebro Delta microbial mats (Tarragona, Spain). One of these

50 microorganisms, *Ochrobactrum anthropi* DE2010, was isolated from the
51 microalgae *Scenedesmus* sp. DE2009 consortium from the same ecosystems,
52 and recently was characterized and identified by means of microbiological,
53 biochemical and molecular methods. Furthermore, the analysis of the effect of
54 deprived nitrogen source conditions on this heterotrophic bacterium
55 demonstrate that it is able to overcome this limiting condition through a still
56 unknown *nif*H–independent mechanism, although there were changes in shape,
57 size, and abundance of pleomorphic cells (Villagrasa et al., 2019).

58 The aims of this work are: (i) to evaluate the cytotoxic effect of chromium
59 and the capacity of *Ochrobactrum anthropi* DE2010, growing in axenic cultures,
60 to remove it; (ii) to determine changes in total biomass and cellular viability and
61 in composition and production of EPS in cultures exposed to this metal and (iii)
62 to determine the Cr(III) uptake efficiency of *Ochrobactrum anthropi* DE2010 and
63 its ability to capture chromium(III) extra and/or intracellularly. With this in mind,
64 an analytical multi-approach combining classical microbial plate counts, growth
65 methods, optical microscope techniques, and biochemical and chemical
66 analysis besides high resolution microscopy techniques have been applied.

67 **2. Materials and methods**

68 2.1 Microorganism, chromium(III) stock solutions and culture conditions

69 *O. anthropi* DE2010 (accession number DDBJ/ENA/GenBank,
70 KY575285) isolated from a *Scenedesmus* sp. DE2009 consortium from Ebro
71 Delta microbial mats (Villagrasa et al., 2019) was grown at 27 °C in Luria–
72 Bertani (LB) agar medium, containing tryptone (10.0 g L^{-1}), yeast extract (5.0 g

L^{-1}), NaCl (10.0 g L^{-1}) and agar (15.0 g L^{-1}), and preserved in Cryoinstant® vials (Thermo Fisher Scientific) at -80 ºC.

Chromium(III) stock solution was prepared as $Cr(NO_3)_3 \cdot 9H_2O$ salt (Sigma-Aldrich, Bellefonte, PA, USA). The 2,600 mg L^{-1} (50 mM) Cr(III) stock solution was made by dissolving the exact quantities of $Cr(NO_3)_3$ in double deionized water and sterilized by filtration through a 0.2 µm filter (Millipore, Merck Millipore). The Cr(III) working concentrations of 0 (control experiment), 0.5, 2, 5, 7, and 10 mM (equivalent to 0, 26, 104, 260, 364, and 520 mg L^{-1}, respectively) were obtained by serial dilution. The Cr(III) stock and serial working solutions were prepared just before use and its pH were adjusted at 6.5.

Unpolluted (0 mM) and polluted (0.5, 2, 5, 7 and 10 mM) cultures were prepared at the same conditions in the following manner: 2 mL of a 24 h culture of *O. anthropi* DE2010 grown in LB (OD_{600} between 1.4-1.6, approximately 10^{10} cfu mL^{-1}) was inoculated into 18 mL of LB liquid medium with the different tested Cr(III) concentrations. These cultures were used for all experiments and were incubated in an orbital shaker (Infors HT, Ecotron) (150 rpm) at 27 ºC for 24 h. Triplicate cultures were grown for each heavy metal concentration.

2.2 Bacterial plate counts and growth curves

To determine the concentration of bacterial cells, 0.1 mL from 24 h cultures grown at different Cr(III) concentrations were spread onto LB agar plates also supplemented with the same final chromium working concentrations:

0, 0.5, 2, 5, 7, and 10 mM. In addition, in order to evaluate the number of dormant *O. anthropi* DE2010 cells, 0.1 mL from each 24 h culture polluted with Cr(III) was spread onto new LB agar plates without Cr(III). The plates were incubated at 27 ºC for 2 d in darkness. The viability counts were expressed in cfu/mL, and 8 replicates were performed for each experiment. The dormant cell counts were determined using the following formula (Sachidanandham et al., 2009):

$$\mathbf{DC} = \mathbf{[100 - (\frac{CC}{CC + RC} x100)]}$$

where DC is the dormant cells relative ratio; CC is the cultivable cells grown with Cr (III) count (cfu mL^{-1}) and RC is the resurrected cells count (cfu mL^{-1}) and corresponds to the difference between cfu mL^{-1} obtained without and with Cr (III).

For growth curve measurements, *Ochrobactrum anthropi* DE2010 culture was grown in LB medium at 27 °C for 24 h in the dark. After this incubation time, a 96-well microplate was prepared by inoculating 20 µL of the above-mentioned over-night culture in microplate columns 2, 4, 6, 8, 10, and 12 filling all the wells. Working Cr(III) concentrations 0, 0.5, 2, 5, 7, and 10 mM at a final volume of 200 µL were used. Blank media samples were considerate by adding bacteria-free LB medium uncontaminated and contaminated with Cr(III) using the same working concentrations in microplate columns 1, 3, 5, 7, 9, and 11, respectively. OD (λ = 600 nm) was measured every 30 min during 24 h with a microtiter plate photometer (Thermo Scientific Variokan® Flash, Waltham, USA). Before each measurement, microtiter plate was shaken for 5 s at 120 rpm. Eight replicates were analyzed for each heavy metal concentration.

123

124 2.3 Cell viability and biomass analysis by Confocal Laser Microscopy (CLSM)

125 Biomass and viability of *O. anthropi* DE2010 cells at different Cr(III)
126 concentrations were determined according to the fluorochromes-confocal laser
127 scanning-image analysis method (FLU-CLSM-IA) described by Puyen et al.
128 (2012a) with some modifications introduced for this particular study. This
129 method combined the use of specific fluorochromes, CLSM, and image analysis
130 using the ImageJ/FIJI v.1.46r software (Schneider et al., 2012).

131

132 For this experiment, 1 mL from each 24 h culture contaminated with a
133 different Cr(III) working concentration was centrifuged at 2000x*g* for 10 min at 4
134 ºC (Eppendorf 5804R refrigerated centrifuge). Then, the obtained pellets were
135 stained with a mixture of 100 µL of two fluorochromes, SYTOX® Green (5 µM)
136 and Hoechst 33342 (64.9 µM) for 30 min at room temperature in the dark.
137 Subsequently, 25 µL of these stained pellets were smeared onto Polylysine®
138 slides (ThermoFisher Scientific, USA), producing a sticky surface and
139 preventing cell movement, mounted in BacLight mounting oil (ThermoFisher
140 Scientific, USA) and immediately covered and sealed with coverslips (24x24
141 mm). Stained cells were observed with a confocal microscope (Leica TCS SP5;
142 Leica Microsystems CMS GmbH, Mannheim, Germany) using a HCX PL APO
143 lambda blue 63.0x1.40 OIL UV at 2 zoom. In this study, *xyz* CLSM images were
144 taken in a sequential scan in two channels to distinguish the fluorescence
145 emitted by Hoechst 33342 (414-485 nm) and SYTOX Green (515-580 nm),
146 respectively. In order to differentiate between living and dead cells, they were
147 stained with Hoechst 333429 or SYTOX Green respectively, blue (live cells) and

148 green (dead cells) pseudo-colors were used. In each bacterial culture, once the
149 20 blue and green CLSM images (1024x1024 pixels) were acquired, the
150 corresponding CLSM binary images (black/white) were generated by means of
151 the ImageJ/FIJI v.1.46r program. In addition, Voxel counter plugin of this
152 software was applied to assess the cellular viability and biomass at each Cr(III)
153 concentration (Puyen et al., 2012a).
154
155 2.4 Extraction and Biochemical analysis of the total EPS
156 Total EPS of *O. anthropi* DE2010 from all analyzed cultures were
157 extracted using the physico-chemical method described by Adav and Lee
158 (2008), with some modifications. For this analysis, 20 mL from each
159 contaminated (0.5, 2, 5, 7, and 10 mM Cr(III)), and non-contaminated (control)
160 culture were centrifuged at 2000x*g* for 10 min at 4 ºC (Eppendorf 5804R
161 refrigerated centrifuge), and pellets were resuspended in 10 mL of sterile
162 double deionized water. Cellular suspensions were mixed with 60 µL of ultra-
163 pure formamide (ThermoFisher Scientific, USA) and incubated on ice for 60
164 min. Then, 4 mL of 1N NaOH was added and the resulting mixtures were
165 incubated for 40 min on ice, and afterward were subjected to ultrasound at 120
166 W for 5 min on ice in an ultrasonic bath (Sonorex, Bandelin). All sonicated
167 suspensions were centrifuged at 10000x*g* for 20 min at 4 ºC. The supernatants
168 obtained were filtered, to avoid the presence of cells, through 0.22 µm pore size
169 filters (Millipore, Merck Millipore) to collect the total EPS. Aliquots of 5 mL of
170 each of the EPS extracts were stored at -20 ºC until further analysis.
171 Biochemical composition of each EPS extract was determined using various
172 colorimetric methods as follows: total carbohydrate content with the phenol–

sulphuric acid method (Dubois et al., 1956), using glucose (1 mg mL^{-1}, Merck) as standard; protein content by the Bradford method (Bradford, 1976), with bovine serum albumin (2 mg mL^{-1}, Pierce) as standard, and the uronic acids content by the *m*-hydroxyphenyl method (Kintner and Van Buren, 1982), using galacturonic acid (1 mg mL^{-1}, Fluka) as standard. The cell lysis caused by EPS extraction was evaluated by quantification of the DNA present in the extracts by the diphenylamine colorimetric method (Burton, 1956) using salmon sperm DNA (1 mg mL^{-1}, Sigma) as standard. Low content of DNA (1-1.2%) indicates that the EPS extracted are not contaminated by intracellular substances (Liu and Fang, 2002). A total of 15 replicates for each EPS extract were analyzed, with the aid of a Beckman Coulter DU® 730 spectrophotometer (Beckman Coulter, Harbor Blvd., Fullerton CA, USA). All calculations were expressed in ppm (parts per million) corresponding to 1 microgram of EPS component (protein, total carbohydrates or uronic acid) per milliliter of total EPS extract (μg mL^{-1}).
On the other hand, the production of EPS was expressed as a percentage of the total concentration of EPS in relation to cell concentration.

2.5 Inductively Coupled Plasma Optical Emission Spectrometer (ICP-OES)

Cr (III) removal capacity of *O. anthropi* DE2010 was analyzed by ICP-OES and the specific metal removal (*q*), expressed as mg of chromium/g of dry weight, was calculated using the following formula (Chakravarty and Banerjee, 2012):

$$\mathbf{q} = \frac{\mathbf{V(Ci - Cf)}}{\mathbf{m}}$$

where V is the sample volume (L); Ci and Cf are the initial and final metal concentrations (mg L^{-1}), and m is the dry culture biomass (g).

198

199 After 24 h, *O. anthropi* DE2010 cultures growing at each tested
200 concentration were centrifuged at 2000x*g* for 10 min at 4 ºC (Eppendorf 5804R
201 refrigerated centrifuge). Samples from the resulting supernatants and liquid
202 samples from the initial Cr(III) working concentrations (without microorganism)
203 were analyzed by ICP-OES. Pellets were resuspended in 10 mL of sterile
204 double deionized water and the corresponding EPS extracts were obtained
205 using the same method as that described above (Adav and Lee, 2008). These
206 extracts and samples from the same cellular suspensions but without EPS were
207 also analyzed by ICP-OES, in order to detect the presence of chromium
208 immobilized into the cells. Before chemical assays, all samples were digested
209 with HNO_3 in a 600 W microwave digestion system to remove all organic
210 matter. Chromium analysis at 267.716 nm was carried out on the resultant
211 digestions using an ICP-OES spectrometer Optima 4300DV (Perkin Elmer LLC,
212 761 Main Avenue, Norwalk, USA), in quadruplicate assays.
213

214 2.6 Energy dispersive X-ray spectroscopy (EDX) analysis coupled to Scanning
215 transmission electron microscope (STEM) imaging

216 Metal sorption capability of *O. anthropi* DE2010 was confirmed by STEM
217 EDX. Samples were prepared following the TEM-EDX protocol described by
218 Maldonado et al. (2010). To this end, a sample from each 24 h culture
219 contaminated with a Cr(III) working concentration was centrifuged at 4000x*g* for
220 5 min at 4 ºC (Eppendorf 5804R refrigerated centrifuge). The resulting pellets
221 were included in soft agar and subsequently fixed in 2.5% glutaraldehyde
222 diluted in Millonig phosphate buffer (Millonig, 1961) for 2 h and washed four

times (15 min) in the same buffer. Then samples were post-fixed in 1% OsO_4 at 4 °C for 2 h and washed again in the same buffer. They were then dehydrated in a graded series of acetone (50, 70, 90, 95, and 100%), and embedded in Spurr's resin. Semi-fine sections (200 nm thick) were mounted on a titanium grid covered with a thin carbon layer without additional staining (lead citrate and uranyl acetate). High angle annular dark field scanning transmission electron microscopy (HAADF-STEM) images and STEM EDX profiles were acquired using a FEI Tecnai G2 F20 microscope operated at 200 kV and equipped with an EDAX super ultra-thin window (SUTW) X-ray detector (FEI, Hillsboro, Oregon, USA).

2.7 Data analysis

Statistical analysis was carried out by one-way analysis of variance (ANOVA) and Tukey multiple comparison *post-hoc* test. Significant differences in ANOVA and Tukey's test were accepted at $p \leq 0.05$. The analyses were performed using SPSS software (version 20.0 for Windows 7).

3. Results and discussion

In this study, several analytical methods were applied to batch cultures in order to evaluate the cytotoxic effect of Cr(III) on *O. anthropi* DE2010, and the capacity of this bacterium to remove it.

3.1 Changes in plate counts, cell viability and biomass

The changes in plate counts, growth curves, cell viability, and biomass in the presence of chromium are shown in Figure 1 (Log_{10} cfu mL^{-1} of total and

cultivable cells, and growth curves), and Figure 2 (FLU-CLSM-IA imaging, live and dead cells%, mg C $(cm^3)^{-1}$, and DC%). The effect of Cr(III) on *O. anthropi* DE2010 varied significantly depending on the concentration, although is more evident at the highest metal concentrations. This is evidenced by a reduction in the number of cfu mL^{-1}, cell viability and biomass, and an increase in DC% and duplication time.

The maximum values of the four biological parameters were obtained at 0 mM Cr(III) ($9.26x10^9$ cfu mL^{-1} of cultivable cells, 4.02 h duplication time, 99.82% of live cells and 46.76 mg C $(cm^3)^{-1}$ of biomass) and the minimum were recovered out for 7 mM (<10 cfu mL^{-1} of cultivable cells, 21 h duplication time, 62.72% of live cells and 3.30 mg C $(cm^3)^{-1}$ of biomass) (Fig 1, and Fig 2). Statistically significant differences were obtained, ranging from 0 mM (control) to 7 mM Cr(III) for viability (F= 213.434) (p <0.05) and biomass (F= 212.253) (p <0.05) results. Using the Tukey multiple comparisons *post-hoc* test, statistically significant differences (p <0.05) were observed among all the metal concentrations tested for cell viability and biomass (Fig 2). On one hand, decreasing values from 0 mM to 7 mM Cr (III) corresponding to reductions in cfu mL^{-1} of 99.99%, cell viability of 37.1% and biomass of 92.94%, were also noted. On the other hand, results of cell viability and biomass at 10 mM Cr(III) could not be determined from FLU-CLSM images due to the formation of cellular aggregates (Fig 2), but a minimal cfu mL^{-1} value was achieved at this concentration (Fig 1). Comparing these results with those obtained by different phototrophic microorganisms, *Scenedesmus* sp. DE2009 and *Geitlerinema* sp. DE2011 (Millach et al., 2015) and *Chroococcus* sp. PCC 9106 (Puyen et al.,

2017) and the yeast *Pichia stipitis* (Yilmazer and Saracoglu, 2008), it can be demonstrated that *O. anthropi* DE2010 shows a great tolerance and resistance to this metal at higher concentrations, even at 10 mM.

It is important to highlight that at 7 mM Cr(III) a high percentage of cells remain alive (FLU-CLSM-IA method) despite minimal viable cells being detected in plate counts. A possible explanation for this fact is the presence of dormant cells (DC) in cultures contaminated with Cr(III) that are unable to grow in plates. Lewis (2010) defined DC as a small sub-population of cells that spontaneously enter a dormant, non-dividing, and resistant state. In this paper, to study the role of DC, 24 h cultures of *O. anthropi* DE2010 grown at the different tested Cr(III) concentrations were also spread onto LB agar without metal (Fig 1A, cfu mL^{-1} of total cells). These results are shown in Figure 2. The number of DC increases as the metal concentration increases. Results were significant at 5 mM Cr(III), with a relative ratio of dormant cells of 96.68%. This can be seen even more clearly at 7 mM and 10 mM Cr(III), where the values were 99.98% and 99.89%, respectively.

3.2 Changes in the EPS composition and production

The results concerning the biochemical analysis of EPS extracts from *O. anthropi* DE2010 cultures grown with Cr(III) at different concentrations are shown in Table 1. Changes in the EPS composition were observed as a response to an increase in Cr(III) concentration. At lower concentrations of Cr(III) (0-2 mM) the major EPS component is carbohydrates (88-89%), followed by proteins (5-7%) and uronic acids (3-5%). However, at 5 mM Cr(III) the most

297 drastic metal effect was assessed. At this concentration, a considerable
298 increase of 37.88% in proteins was observed in contrast to a significant
299 reduction in 35.45% in carbohydrates, with as well as a slight decrease in uronic
300 acid content. Guibaud et al. (2003) demonstrated that the protein played a
301 major role in the complexation of metal ions and the number of binding sites
302 (alcohol, carboxyl and amino groups) for heavy metals. This change in the EPS
303 composition coincide with that described by Seng et al. (2005), who indicate
304 that the content of extracellular proteins increased when bacteria were grown in
305 adverse environmental conditions, and Yin et al. (2011), who report that the
306 presence of heavy metals resulted in a higher production of proteins than total
307 carbohydrates and uronic acids in the EPS. A decreasing value in
308 carbohydrates and proteins content is observed from 7 mM Cr(III), reaching a
309 similar value between both EPS components, although a slight increase was
310 observed at 10 mM, as result of cell aggregation. Regarding the uronic acids
311 content, in this study its role in *O. anthropi* DE2010 is less clear, although
312 different authors have been demonstrated the active role of this EPS
313 components in heavy metals chelation (Guibaud et al., 2005; Morillo Pérez et
314 al., 2008; Pal and Paul, 2008). The results showed in Table 1 demonstrated that
315 the concentration of uronic acid decreases from 0 to 5 mM and it is maintained
316 at higher Cr(III) concentrations, especially at 7 mM, when the carbohydrates
317 and proteins reach the lowest values. This data coincides with the formation of
318 cellular aggregates, which probably indicates that under these conditions,
319 uronic acid could contribute to chromium immobilization. Statistically significant
320 differences were found among all the metal concentrations assayed for
321 carbohydrates ($F= 271.15$) ($p < 0.05$), proteins ($F= 471.14$) ($p < 0.05$), and uronic

322 acids (F= 130.28) (p <0.05). Using the Tukey multiple comparisons post-hoc
323 test, statistically significant differences (p <0.05) were labelled in Table 1.
324
325 As regards the EPS production, a maximum increase in EPS
326 concentration in relation to cell concentration (7.82%) was obtained from 0 mM
327 (10.17%) to 5 mM (17.99%) Cr(III) coinciding with the increment in the protein
328 content. It is well known that the EPS generally contains high molecular weight
329 compounds with charged functional groups with adsorptive and adhesive
330 properties. These functional groups provide binding sites for heavy metals, as
331 demonstrated by Decho (1990) and more recently by other authors (More et al.,
332 2014; Yue et al., 2015). These results could explain the increase in total amount
333 of EPS at high concentrations of Cr(III) in *O. anthropi* DE2010.
334
335 As previously mentioned the most important cytotoxic effect of Cr(III) on
336 *O. anthropi* DE2010 is produced at 5 mM Cr(III). At this concentration, the
337 percentage of dead cells increases, provoking a drop in viability and biomass.
338 This is linked to an enhancement in the cellular synthesis of EPS by *O. anthropi*
339 DE2010 to protect the cells themselves from chromium toxicity, increasing, in
340 turn, the protein content and reducing the amount of carbohydrate and uronic
341 acids.
342
343 3.3 Removal capacity for Cr(III) of *O. anthropi* DE2010
344 Quantitative chemical data for the ability of *O. anthropi* DE2010 cells to
345 capture Cr(III) and the corresponding cellular uptake efficiency (q) are shown in
346 Table 2. These results indicate that there is a strong correlation between the

initial concentration of metal and the total of chromium taken from the cells, reaching maximum values of removal of 40.83% at 7 mM and of 38.38% at 10 mM Cr(III). In addition, practically all the chromium removed was detected inside the cells (cytoplasm), with values ranging between 97% and 99%, depending on the metal concentration, with the rest of the metal being found in the EPS extracts (1-3%). These results indicate that *O. anthropi* DE2010 is able to immobilize chromium in both the EPS and the cytoplasm of the cells. The *q* values also increase by increasing the initial metal concentration, and a maximum value of 950 mg g^{-1} was reached at 10 mM Cr(III). However, the most notable increase in *q* values (590 mg g^{-1}) was observed from 5 mM to 7 mM Cr(III). The highest *q* value reported here could be related to the cellular aggregation monitored by CLSM imaging at 10 mM. This cellular organization is more efficient to capture Cr(III) and to protect the cells from the cytotoxic effect of the metal than the individual cells observed at the other metal concentrations. Statistically significant differences for *q* values (F= 1,596.45) (p <0.05) were found among all the metal concentrations assayed. Using the Tukey multiple comparisons *post-hoc* test, statistically significant differences (p <0.05) were observed from 5 mM Cr(III) and were included in Table 2. The specific removal efficiency (*q*) of *O. anthropi* DE2010 is higher with respect to those obtained by other prokaryotic: 120 mg g^{-1} in *Sphaerotilus natans* (Solisio et al., 2000), 185 mg g^{-1} in *Spirullina* sp. (Chojnacka et al., 2005), and 14.28 mg g^{-1} in *Rhodococcus opacus* (Calfa et al., 2008); and eukaryotic microorganisms: 11.30 mg g^{-1} in *Saccharomyces cerevisiae* (Ksheminska et al., 2005), and 41.18 mg g^{-1} in *Chlorella miniata* (Han et al., 2006). For this reason, it can be considered that *O. anthropi* DE2010 show a higher capacity to sequestrate

chromium into the cells than other microorganisms and is, therefore, a great candidate to bioremediate natural/artificial environments polluted with chromium.

3.4 Cr(III) localization at cellular structure level

Electron microscopy imaging, SEM and TEM, have become a crucial tool to visualize the ultrastructure of microorganisms (Rachel et al., 2010; Golding et al., 2016; Solé et al., 2019) and coupled to an EDX detector to analyze the elemental composition and its distribution in the samples (Maldonado et al., 2011, Burgos et al., 2013; Coreño-Alonso et al., 2014; Millach et al., 2015; Povedano-Priego et al., 2017). Although, these techniques have been very useful in this regard, we applied for the first time the HAADF-STEM EDX for locating, at the nanoscale level, heavy metals immobilized on different cellular structures (Fig 3) evidencing whether specific microorganisms have a capacity to immobilize them inside and/or outside cells in the same semi-fine section.

HAADF-STEM images exhibited discernible changes (changes in cell morphology, an increase in bright inclusions, and the appearance of cellular pleomorphic forms) in cells (Fig 3 A1, B1, and C1) due to the Cr (III), mainly at the highest concentration (10 mM Cr(III)). EDX microanalyses shows that chromium was not detectable, either externally or internally, in control samples (0 mM) and up to 2 mM Cr(III). However, results obtained from 5 mM to 10 mM indicated that the chromium signal was detected in the cellular structure. Figures 3 A2, B2, and C2 show the STEM EDX chromium and phosphorous composition line profiles that were taken along a bright inclusion from a semi-

fine section micrograph of *O. anthropi* DE2010 grown at 0, 5, and 10 mM Cr(III). When compared the image intensity profile, with an increased signal in the bright inclusion, it is clear that the most part of chromium was located in the bright inclusions, together with an important phosphorous signal, and secondarily on the cellular surface at the EPS level.

It is known that microorganisms play an important role in heavy metal immobilization processes (Cheng et al., 2010) either at extra-cellular (biosorption) and/or intra-cellular (bioaccumulation) levels (Guibaud et al., 2005; Guine et al., 2006; Kothe et al., 2010; Puyen et al., 2012b; Esteve et al., 2013; Burgos et al., 2013; Gutiérrez-Corona et al., 2016). On the other hand, Velásquez and Dussan, (2009) demonstrated the relation between external capture and passive process (live or dead cells) and internal bioaccumulation and active process (live cells).

The present STEM EDX results demonstrate that *O. anthropi* DE2010 accumulates Cr(III) externally in EPS, and internally mainly in cytoplasmic polyphosphate inclusions. Therefore, the chromium removal via sorption and accumulation mechanisms in this bacterium was demonstrated using STEM EDX.

Conclusions

Our results indicate that *O. anthropi* DE2010 is able to (i) tolerate and resist the presence of high Cr(III) concentrations, showing changes in production and EPS composition and increasing the number of dormant cells,

(ii) capture chromium at higher removal efficiencies, and (iii) immobilize it mainly inside the cell in polyphosphate inclusions (bioaccumulation process), as well as externally in the EPS (biosorption process).

As a future perspective, *O. anthropi* DE2010 could be considered as a potential agent for bioremediation in Cr(III) contaminated environments since it shows a great ability to tolerate and efficiently remove Cr(III) from polluted cultures.

Acknowledgments

We express our thanks for the assistance of the UAB staff of Servei de Micròscopia (http://sct.uab.cat/microscopia/) in particular Dr Alejandro Sanchez-Chardi, the UAB Servei de Anàlisi Química (http://sct.uab.cat/saq/) especially Dr Ignacio Villarroya. We also appreciate the help of Cristina Sosa and the valuable comments and suggestions of Diana Gutiérrez, Irene López-Gómez, and Estefania Solsona. This research was supported by the following grants: FONCICYT (Ref. 95887), Ministerio de Economía y Competitividad (Refs. CTQ2014-54553-C3-2-R and CGL2008-01891) and UAB postgraduate scholarship to EV. The ICN2 is supported by the Severo Ochoa (MINECO, grant no. SEV-2017-0706) and CERCA programmes.

Conflicts of interest

The authors declare no conflict of interests**.**

References:

442 Adav, S.S., Lee, D.J., 2008. Extraction of extracellular polymeric substances
443 from aerobic granule with compact interior structure. J. Hazard. Mater. 154
444 (1-3), 1120-1126. https://doi.org/10.1016/j.jhazmat.2007.11.058.

445 Balk, E.M., Tatsioni, A., Lichtenstein, A.H., Lau, J., Pittas, A.G., 2007. Effect of
446 chromium supplementation on glucose metabolism and lipids: a
447 systematic review of randomized controlled trials. Diabetes Care 30 (8),
448 2154–2163. https://doi.org/10.2337/dc06-0996.

449 Bhattacharya, A., Dey, P., Gola, D., Mishra, A., Malik, A., Patel, N., 2015.
450 Assessment of Yamuna and associated drains used for irrigation in rural
451 and peri-urban settings of Delhi NCR. Environ. Monit. Assess. 187, 4146.
452 https://doi.org/10.1007/s10661-014-4146-2.

453

454 Bradford, M., 1976. A rapid and sensitive method for the quantification of
455 microgram quantities of protein utilizing the principle of protein– dye
456 binding. Anal. Biochem. 72, 248–254. https://doi.org/10.1016/0003-
457 2697(76)90527-3.

458

459 Burgos, A., Maldonado, J., De los Rios, A., Solé, A., Esteve, I., 2013. Effect of
460 copper and lead on two consortia of phototrophic microorganisms and
461 their capacity to sequester metals. Aquat. Toxicol. 140–141, 324–336.
462 https://doi.org/10.1016/j.aquatox.2013.06.022.

463

464 Burton, K., 1956. A study of the conditions and mechanism of the
465 diphenylamine reaction for the colorimetric estimation of deoxyribonucleic
466 acid. Bioch. 62, 315-323.

Calfa, BA., Torem, ML., 2008. On the fundamentals of Cr(III) removal from liquid streams by a bacterial strain. Miner. Eng. 21 (1), 48-54. https://doi.org/10.1016/j.mineng.2007.08.001.

Chakravarty, R., Banerjee, P.C., 2012. Mechanism of cadmium binding on the cell wall of an acidophilic bacterium. Bioresour.Technol.108, 176-183. https://doi.org/10.1016/j.biortech.2011.12.100.

Cheng, Y., Yan, F., Huang, F., Chu, W., Pan, D., Chen, Z., Zheng, J., Yu, M., Lin Z., Wu, Z., 2010. Bioremediation of Cr (VI) and immobilization as Cr (III) by *Ochrobactrum anthropi.* Environ. Sci. Technol. 44 (16), 6357–6363. https://doi.org/10.1021/es100198v.

Chojnacka, K., Chojnacki, A., Górecka, H., 2005. Biosorption of Cr^{3+}, Cd^{2+} and Cu^{2+} ions by blue–green algae *Spirulina* sp.: kinetics, equilibrium and the mechanism of the process. Chemosphere 59 (1), 75-84. https://doi.org/10.1016/j.chemosphere.2004.10.005.

Coreño-Alonso, A., Solé, A., Diestra, E., Esteve, I., Gutiérrez-Corona, J.F., Reyna López, G.E., Fernández, F.J., Tomasini, A., 2014. Mechanisms of interaction of chromium with *Aspergillus niger* var tubingensis strain Ed8. Bioresour. Technol. 158, 188–192. https://doi.org/10.1016/j.biortech.2014.02.036.

Decho, A.W., 1990. Microbial exopolymer secretions in ocean environments: Their role(s) in food webs and marine processes. Oceanogr. Mar. Biol. Annu. Rev. 28 (7), 73-153. https://doi.org/10.1016/j.carbpol.2018.04.126.

Dubois, M., Gilles, K.A., Hamilton, J.K., Rebers, P.A., Smith, F., 1956. Colorimetric method for determination of sugars and related substances. Anal. Chem. 28 (3), 350-356.

Esteve, I., Maldonado, J., Burgos, A., Diestra, E., Burnat, M., Solé, A., 2013. Confocal laser scanning and electron microscopic techniques as powerful tools for determining the in vivo effect and sequestration capacity of lead in cyanobacteria. Cyanobacteria: Ecology, Toxicology and Management.

Evert, A.B., Boucher, J.L.B., Cypress, M., Dunbar, S.A., Franz, M.J., Mayer-Davis, E.J., Neumiller, J.J., Nwankwo, R., Verdi, C.L., Urbanski, P., Yancy, W.S., 2013. Nutrition therapy recommendations for the management of adults with diabetes. Diabetes Care 36 (11), 3821-3842. http://doi.org/10.2337/dc13-2042.

Feng, S., Mai, B., Wei, G., Wang, X., 2012. Genotoxicity of the sediments collected from Pearl River in China and their polycyclic aromatic hydrocarbons (PAHs) and heavy metals. Environ. Monit. Assess. 184, 5651–5661. http://doi.org/10.1007/s10661-011-2369-z.

516 Figgitt, M., Newson, R., Leslie, I.J., Fisher, J., Ingham, E., Case, C.P., 2010.
517 The genotoxicity of physiological concentrations of chromium (Cr(III) and
518 Cr(VI)) and cobalt (Co(II)): An in vitro study. Mutat. Res. 688, 53–61.
519 http://doi.org/10.1016/j.mrfmmm.2010.03.008.
520
521 Francisco, R., de Abreu, P., Plantz, B.A., Schlegel, V.L., Carvalho, R.A.,
522 Vasconcelos-Morais, P., 2011. Metal-induced phosphate extracellular
523 nanoparticulate formation in *Ochrobactrum tritici* 5bvl1. J. Hazard. Mater.
524 198, 31-39. https://doi.org/10.1016/j.jhazmat.2011.10.005.
525
526 Golding, C.G., Lamboo, L.L., Beniac, D.R., Booth, T.F., 2016. The scanning
527 electron microscope in microbiology and diagnosis of infectious disease.
528 Sci. Rep. 6, 26516. https://doi.org/10.1038/srep26516
529
530 Greenwood, N.N., Earnshaw, A., 1997. Chemistry of the elements, 2nd ed.
531 Butterworth–Heinemann, Oxford.
532
533 Guibaud, G., Tixier, N., Bouju, A., Baudu, M., 2003. Relation between
534 extracellular polymers' composition and its ability to complex Cd, Cu and
535 Pb. Chemosphere 52(10),1701-1710. https://doi.org/10.1016/S0045-
536 6535(03)00355-2.
537
538 Guibaud, G., Comte, S., Bordas, F., Dupuy, S., Baudu, M., 2005. Comparison
539 of the complexation potential of extracellular polymeric substances (EPS),
540 extracted from activated sludges and produced by pure bacteria strains,

for cadmium, lead and nickel. Chemosphere 59 (5), 629-638. http://doi.org/10.1016/j.chemosphere.2004.10.028.

Guiné, V., Spadini, L., Sarret, G., Muris, M., Delolme, C., Gaudet, J.P., Martins, J.M.F., 2006. Zinc sorption to three gram-negative bacteria: combined titration, modeling, and EXAFS study. Environ. Sci. Technol. 40 (6),1806–1813. https://doi.org/10.1021/es050981l.

Gupta, S.K., Chabukdhara, M., Kumar, P., Singh, J., Bux, F., 2014. Evaluation of ecological risk of metal contamination in river Gomti, India: a biomonitoring approach. Ecotoxicol. Environ. Saf. 110, 49–55. http://doi.org/10.1016/j.ecoenv.2014.08.008.

Gutiérrez-Corona, J.F., Romo-Rodríguez, P., Santos-Escobar, F., Espino-Saldaña, A.E., Hernández-Escoto, H., 2016. Microbial interactions with chromium: basic biological processes and applications in environmental biotechnology. World. J. Microbiol. Biotechnol. 32 (12), 191. https://doi.org/10.1007/s11274-016-2150-0.

Han, X., Wong, YS., Tam, NFY., 2006. Surface complexation mechanism and modeling in Cr(III) biosorption by a microalgal isolate, *Chlorella miniate*. J. Colloid Interface Sci. 303 (2), 365-371. https://doi.org/10.1016/j.jcis.2006.08.028.

565 Ihsanullah, Abbas, A., Al-Amer, A.M., Laoui, T., Al-Marri, M.J., Nasser, M.S.,
566 Khraisheh, M., Atieh, M.A., 2016. Heavy metal removal from aqueous
567 solution by advanced carbon nanotubes: Critical review of adsorption
568 applications. Sep. Purif. Technol. 157 (8), 141-161.
569 https://doi.org/10.1016/j.seppur.2015.11.039.

570 Kimbrough, D.E., Cohen, Y., Winer, A.M., Creelman, L., Mabuni, C., 1999. A
571 Critical assessment of chromium in the environment. Crit. Rev. Environ.
572 Sci. Technol. 29 (1), 1-46. https://doi.org/10.1080/10643389991259164.

573 Kintner, P.K., van Buren, J.P.,1982. Carbohydrate Interference and Its
574 Correction in pectin analysis using the *m*-Hydroxydiphenyl method. J.
575 Food Sci. 47, 756-759. https://doi.org/10.1111/j.1365-
576 2621.1982.tb12708.x.

577 Kothe, E., Dimkpa, C., Haferburg, G., Schmidt, A., Schmidt, A., Schütze, E.,
578 2010. Streptomycete heavy metal resistance: extracellular and intracellular
579 mechanisms, in: Sherameti, I., Varma, A., (Eds.). Soil Heavy Metals, Soil
580 Biology. https://doi.org/10.1007/978-3-642-02436-8_10.
581

582 Ksheminska, H., Fedorovych, D., Babyak, L., Yanovych, D., Kaszycki, P.,
583 Koloczek, H., 2005. Chromium (III) and (VI) tolerance and bioaccumulation
584 in yeast: A survey of cellular chromium content in selected strains of
585 representative genera. Process Biochemistry. 40, 1565-1572.
586 https://doi.org/10.1016/j.procbio.2004.05.012.

587 Kusiak, R.A., Ritchie, A.C., Springer, J., Muller, J., 1993. Mortality from stomach
588 cancer in Ontario miners. Br. J. Med. 50,117–126.

Lewis K., 2010. Persister Cells. Annu. Rev. Microbiol. 64, 357–372.

Liu, H., Fang, H.P.H., 2002. Extraction of extracellular polymeric substances (EPS) of sludges. J. Biotechnol. 95 (3), 249-256. https://doi.org/10.1016/S0168-1656(02)00025-1.

Maldonado, J., Diestra, E., Domènech, A.M., Villagrasa, E., Puyen, Z.M, Esteve, I., Solé, A., 2010. Isolation and identification of a bacterium with high tolerance to lead and copper from a marine microbial mat in Spain. Ann. Microbiol. 60 (1), 113-120. https://doi.org/10.1007/s13213-010-0019-2.

Maldonado, J., Solé, A., Puyen, Z.M., Esteve, I., 2011. Selection of bioindicators to detect lead pollution in Ebro delta microbial mats, using high-resolution microscopic techniques. Aquat.Toxicol.104, 135–144. http://doi.org/10.1016/j.aquatox.2011.04.009.

Manahan, S.E., 2009. Environmental chemistry, 9th edition. Boca Raton: CRC Press, Florida.

Millach, L., Solé, A., Esteve, I., 2015. Role of *Geitlerinema* sp. DE2011 and *Scenedesmus* sp. DE2009 as bioindicators and immobilizers of chromium in a contaminated natural environment. BioMed Research International, Article ID 519769. https://doi.org/10.1155/2015/519769.

Millonig, G.,1961. A modified procedure for lead staining of thin sections. J Biophys. Biochem. Cytol. 11 (3), 736–739.

Mohana, D., Pittman, C.U., 2006. Activated carbons and low cost adsorbents for remediation of tri- and hexavalent chromium from water. J. Hazard. Mater. 137 (2), 762-811. https://doi.org/10.1016/j.jhazmat.2006.06.060.

More, T.T., Yadav, J.S.S., Yan, S., Tyagi, R.D., Surampalli. R.Y., 2014. Extracellular polymeric substances of bacteria and their potential environmental Applications. J. Environ. Manage. 144, 1-25. https://doi.org/10.1016/j.jenvman.2014.05.010.

Morillo Pérez, J.A., García-Ribera, R., Quesada, T., Aguilera, M., Ramos-Cormenzana, A., Monteoliva-Sánchez M., 2008. Biosorption of heavy metals by the exopolysaccharide produced by *Paenibacillus jamilae*. World J. Microbiol. Biotechnol. 24, 2699. https://doi.org/10.1007/s11274-008-9800-9.

Nziguheba, G., Smolders, E., 2008. Inputs of trace elements in agricultural soils via phosphate fertilizers in European countries. Sci. Total. Environ. 390 (1), 53-57. https://doi.org/10.1016/j.scitotenv.2007.09.031.

637 Pal, A. and Paul, A.K., 2008. Microbial extracellular polymeric substances:
638 central elements in heavy metal bioremediation. Indian J. Microbiol. 48,
639 49-64.
640
641 Povedano-Priego, C., Martín-Sánchez, I., Jroundi, F., Sánchez-Castro, I.,
642 Merroun, M.L., 2017. Fungal biomineralization of lead phosphates on the
643 surface of lead metal. Miner. Eng. 106, 46–54.
644 https://doi.org/10.1016/j.mineng.2016.11.007.
645
646 Puyen, Z.M., Villagrasa, E., Maldonado, J., Esteve, I., Solé, A., 2012a. Viability
647 and biomass of *Micrococcus luteus* DE2008 at different salinity
648 concentrations determined by specific fluorochromes and CLSM-image
649 analysis. Curr. Microbiol. 64 (1), 75-80. https://doi.org/10.1007/s00284-
650 011-0033-z.
651
652 Puyen, Z.M., Villagrasa, E., Maldonado, J., Diestra, E., Esteve, I., Solé, A.,
653 2012b. Biosorption of lead and copper by heavy-metal tolerant
654 *Micrococcus luteus* DE2008. Bioresour. Technol. 126, 233–237.
655 https://doi.org/10.1016/j.biortech.2012.09.036.
656
657 Puyen, Z. M., Villagrasa, E., Millach, L., Esteve, I., Maldonado, J., Solé, A.,
658 2017. Multi-approach microscopy techniques to evaluate the cytotoxic
659 effect of chromium(III) on the cyanobacterium *Chroococcus* sp. PCC 9106.
660 in: Menendez-Vilas, A. (Ed). Microscopy and imaging science: practical

approaches to applied research and education. Formatex Research Center, Badajoz, pp. 602-609.

Rachel, R., Meyer, C., Klingl, A., Gürster, S., Heimerl, T., Wasserburger, N., Burghardt, T., Küper, U., Bellack, A., Schopf, S., Wirth, R., Huber, H., Wanner G., 2010. Chapter 3 - Analysis of the Ultrastructure of Archaea by Electron Microscopy, Editor(s): Thomas Müller-Reichert. Methods in Cell Biology. Academic Press. Vol(96), pages: 47-69. https://doi.org/10.1016/S0091-679X(10)96003-2.

Sachidanandham, R., Yew-Hoong Gin, K., 2009. A dormancy state in nonspore-forming bacteria. Appl. Microbiol. Biotechnol. 81, 927. https://doi.org/10.1007/s00253-008-1712-y.

Schneider, C.A., Rasband, W.S., Eliceiri, K.W., 2012. NIH Image to ImageJ: 25 years of Image Analysis. Nat. Methods 9 (7), 671–675.

Shanker, A.K., Cervantes, C., Loza-Tavera, H., Avudainayagam, S., 2005. Chromium toxicity in plants. Environ. Int. 31 (5), 739-753. https://doi.org/10.1016/j.envint.2005.02.003.

Sheng, G.P., Yu, H.Q., Yue, Z.B., 2005. Production of extracellular polymeric substances from *Rhodopseudomonas acidophila* in the presence of toxic substances. Appl. Microbiol. Biotechnol. 69 (2), 216-222. https://doi.org/10.1007/s00253-005-1990-6.

Sole, A., Calvo, M.A., Lora, M.J., Sánchez-Chardi, A., 2019. Chapter 12 - Electron microscopy techniques applied to bioremediation and biodeterioration studies with molds. Editor(s): Araceli Tomasini Campocosio and Hector Hugo Leon Santiesteban. Fungal bioremediation: fundamentals and applications. CRC press. pages: 354. https://doi.org/10.1201/9781315205984.

Solisio, C., Lodi, A., Converti, A., Del Borghi, M., 2000.The effect of acid pre-treatment on the biosorption of chromium(III) by *Sphaerotilus natans* from industrial wastewater. Water Res. 34 (12), 3171-3178. https://doi.org/10.1016/S0043-1354(00)00059-2.

Srivastava, S., Thakur, I.S., 2007. Evaluation of biosorption potency of *Acinetobacter* sp. for removal of hexavalent chromium from tannery effluent. Biodegradation 18 (5), 637–646. https://doi.org/10.1007/s10532-006-9096-0.

Suwalsky, M., Castro, R., Villena, F., Sotomayor, C.P., 2008. Cr(III) exerts stronger structural effects than Cr(VI) on the human erythrocyte membrane and molecular models. J. Inorg. Biochem. 102, 842–849. https://doi.org/10.1016/j.jinorgbio.2007.11.020.

709 Velásquez, L., Dussan, J., 2009. Biosorption and bioaccumulation of heavy
710 metals on dead and living biomass of *Bacillus sphaericus*. J. Hazard.
711 Mater. 167 (1-3), 713–6. https://doi.org/10.1016/j.jhazmat.2009.01.044.
712
713 Villagrasa, E., Ferrer-Miralles, N., Millach, L., Obiol, A., Creus, J., Esteve, I.,
714 Solé, A., 2019. Morphological responses to nitrogen stress deficiency of a
715 new heterotrophic isolated strain of Ebro Delta microbial mats.
716 Protoplasma. 256 (1), 105-116. https://doi.org/10.1007/s00709-018-1263-
717 8.
718
719 Xu, X., Zhao, Y., Zhao, X., Wang, Y., Deng, W., 2014. Sources of heavy metal
720 pollution in agricultural soils of a rapidly industrializing area in the Yangtze
721 Delta of China. Ecotoxicol. Environ. Saf. 108, 161–167.
722 https://doi.org/10.1016/j.ecoenv.2014.07.001.
723
724 Yilmazer, P., Saracoglu, N., 2009. Bioaccumulation and biosorption of
725 copper(II) and chromium(III) from aqueous solutions by *Pichia stipitis*
726 yeast. J. Chem. Technol. Biotechnol. 84, 604–610.
727 https://doi.org/10.1002/jctb.2088.
728
729 Yin, Y., Hu, Y., Xiong, F., 2011. Sorption of Cu (II) and Cd (II) by extracellular
730 polymeric substances (EPS) from *Aspergillus fumigates*. Int. Biodeterior.
731 Biodegrad., 65, 1012-1018. https://doi.org/10.1016/j.ibiod.2011.08.001.
732

733 Yue, Z.B., Li, Q., Li, C.C., Chen, T.H., Wang, J., 2015. Component analysis and
734 heavy metal adsorption ability of extracellular polymeric substances (EPS)
735 from sulfate reducing bacteria. Bioresour. Technol. 194, 399-402.
736 https://doi.org/10.1016/j.biortech.2015.07.042.

Table 1 Variations in the production and composition of the EPS of *Ochrobactrum anthropi* DE2010

Cr(III) concentration (mM)	[DNA] (ppm)	[Carbohydrates] (ppm)	[Proteins] (ppm)	[Uronic acids] (ppm)	[Cell co (ppm)
0	0.28 ± 0.02	148.12 ± 4.94	9.98 ± 0.71	8.40 ± 0.71	1640 ± 8
0.5	0.58 ± 0.02**	150.50 ± 2.09	11.95 ± 0.52	6.30 ± 0.34**	1580 ± 1
2	0.91 ± 0.02**$^{++}$	133.28 ± 5.44	11.89 ± 0.88	6.02 ± 0.20**	1505 ± 1
5	1.20 ± 0.02**$^{++\$\$}$	45.36 ± 0.95**$^{++\$\$}$	39.37 ± 0.44**$^{++}$	1.35 ± 0.16**$^{++\$\$}$	485 ± 24
7	0.87 ± 0.03^{a}**$^{++\&\&}$	12.46 ± 0.15**$^{++\$\$\&\&}$	10.72 ± 1.16$^{\&\&}$	0.97 ± 0.07**$^{++\$\$\&\&}$	255 ± 4.6
10	1.27 ± 0.03^{a}**$^{++\$\$\wedge\wedge}$	17.36 ± 0.24**$^{++\$\$\&\&}$	12.47 ± 4.36*$^{\&\&}$	1.37 ± 0.26**$^{++\$\$\wedge\wedge}$	220 ± 4.7

^{a} values out of range indicating cell lysis due to Cr(III)

Data are expressed as mean ±SD (n= 15)

*p <0.05; **p <0.01: 0.5, 2, 5, 7 and 10 mM treatments vs. control (0 mM)

^{+}p <0.05; ^{++}p <0.01: 2, 5, 7, and 10 mM treatments vs. 0.5 mM treatment

$^{\$\$}p$ <0.01: 5, 7, and 10 mM treatments vs. 2 mM treatment

$^{\&\&}p$ <0.01: 7, and 10 mM treatments vs. 5 mM treatment

$^{\wedge\wedge}p$ <0.01: 7 treatment mM vs. 10 mM treatment

Table 2 Removal Cr(III) capacity by *Ochrobactrum anthropi* DE2010 in the EPS and cytoplasm

Cr(III) concentration (mM)	Culture Medium (C_i) (mg L^{-1})	Supernatant (C_f) (mg L^{-1})	Total metal removed (mg L^{-1})	Metal in EPS (mg L^{-1})	Metal in cells without EPS (mg L^{-1})	Dry we (m) (g)
0	0	0	0	0	0	0.033 ±
0.5	24 ± 1.15	16.50 ± 0.57	7.50 ± 1.73	0.20 ± 0.006	7.30 ± 1.71	0.031 ±
2	99 ± 2.30	83.50 ± 1.73	15.50 ± 4.04	0.21 ± 0.010	15.29 ± 4.03	0.030 ±
5	257 ± 2.31	199 ± 3.46	58 ± 1.15	0.52 ± 0.015	57.48 ± 1.14	0.010 ±
7	360 ± 3.46	212.50 ± 2.89	147.50 ± 0.58	1.85 ± 0.045	145.15 ± 0.54	0.005 ±
10	495 ± 9.24	305 ± 8.08	190 ± 8.99	5.10 ± 0.095	184.90 ± 0.90	0.004 ±

Data are expressed as mean ±SD (n= 4)

*p <0.05, **p <0.01: 0.5, 2, 5, 7 and 10 mM treatments vs. control (0 mM)

^{++}p <0.01: 2, 5, 7, and 10 mM treatments vs. 0.5 mM treatment

$^{\$\$}p$ <0.01: 5, 7, and 10 mM treatments vs. 2 mM treatment

$^{\&\&}p$ <0.01: 7, and 10 mM treatments vs. 5 mM treatment

$^{\wedge\wedge}p$ <0.01: 7 treatment mM vs. 10 mM treatment

Figure captions

Figure 1 Growth parameters of *O. anthropi* DE2010 growing at different Cr(III) concentrations. (**A**) Plate counts (cfu mL^{-1}) from total (grown on LB agar without Cr(III)) and cultivable cells (grown on LB agar with Cr(III)). p <0.01**: 0.5, 2, 5, 7, and 10 mM treatments vs. control (0 mM). (**B**) Growth curves at different Cr(III) working concentrations. In both graphics, data are expressed as mean ±SD (n= 8).

Figure 2 Cytotoxic effect of Cr(III) in the *O. anthropi* DE2010 cultures. *p <0.05, **p <0.01: 0.5, 2, 5, and 7 mM treatments vs. control (0 mM). ^{+}p <0.05, ^{++}p < 0.01: 2, 5, and 7 mM treatments vs. 0.5 mM treatment. $^{\$\$}p$ <0.01: 5, and 7 mM treatments vs. 2 mM treatment. Data are expressed as mean ±SD (n= 20).

Figure 3 HAADF STEM analysis of *O. anthropi* DE2010 cells grown at 0 (**A**), 5 (**B**), and 10 mM (**C**) of Cr(III). (**A1**, **B1**, and **C1**) HAADF STEM imaging, and (**A2**, **B2**, and **C2**) HAADF STEM-EDX analysis and line profiles (250 nm) along the black line showing the intensity of the HAADF image (top), phosphorus (middle) and chromium (bottom).

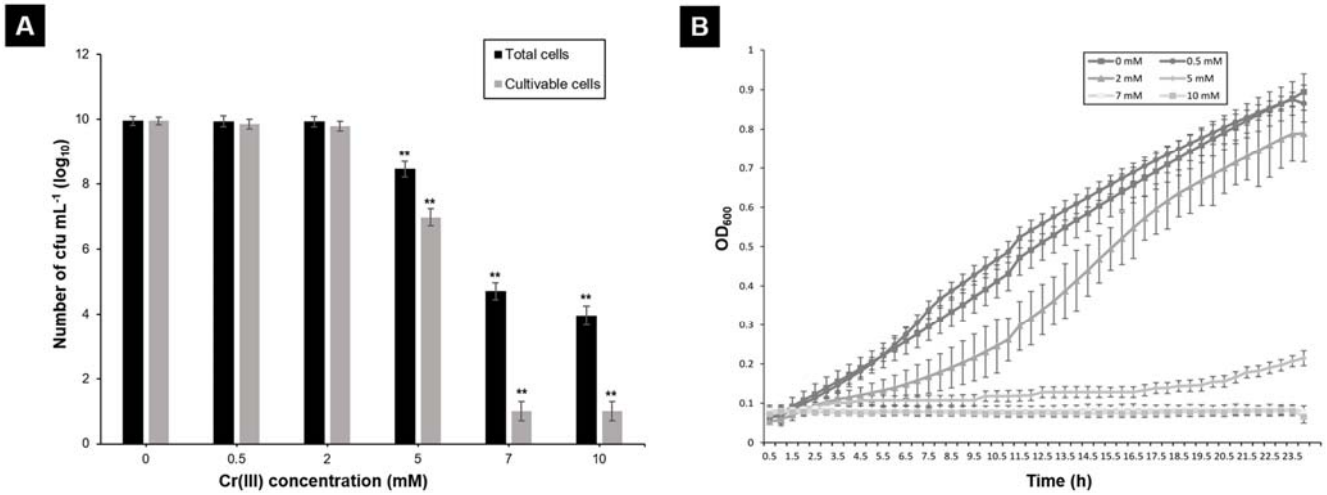
A
Total cells
Cultivable cells
Number of cfu mL-1 (log10)
Cr(III) concentration (mM)
0
0.5
2
5
7
10
B
0 mM
0.5 mM
2 mM
5 mM
7 mM
10 mM
OD600
Time (h)

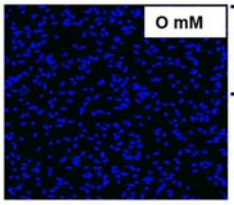

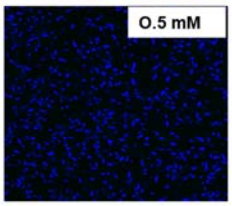

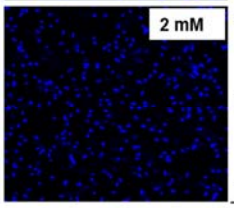

Cr (III) Concentration (mM)	Live cells (%)	Dead cells (%)	Biomass (mg C/ cm^3)	DC (%)
0	99.82 ± 9.13	0.18 ± 0.006	46.76 ± 8.57	0
0.5	99.75 ± 8.17	0.25 ± 0.009	32.69 ± 5.27*	17.04 ± 1.06*
2	99.55 ± 8.11*	0.45 ± 0.012*	27.40 ± 3.83*+	27.95 ± 1.78*++
5	74.21 ± 3.09*++$$	25.79 ± 1.03*++$$	6.38 ± 1.56*++$$	96.68 ± 2.43*++$$
7	62.72 ± 0.85*++$$	37.28 ± 0.43*++$$	3.30 ± 0.40*++$$	99.98 ± 2.76*++$$
10	ND	ND	ND	99.89 ± 3.34*++$$

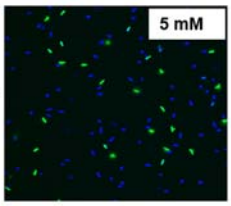

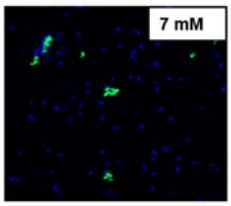

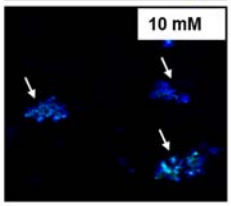

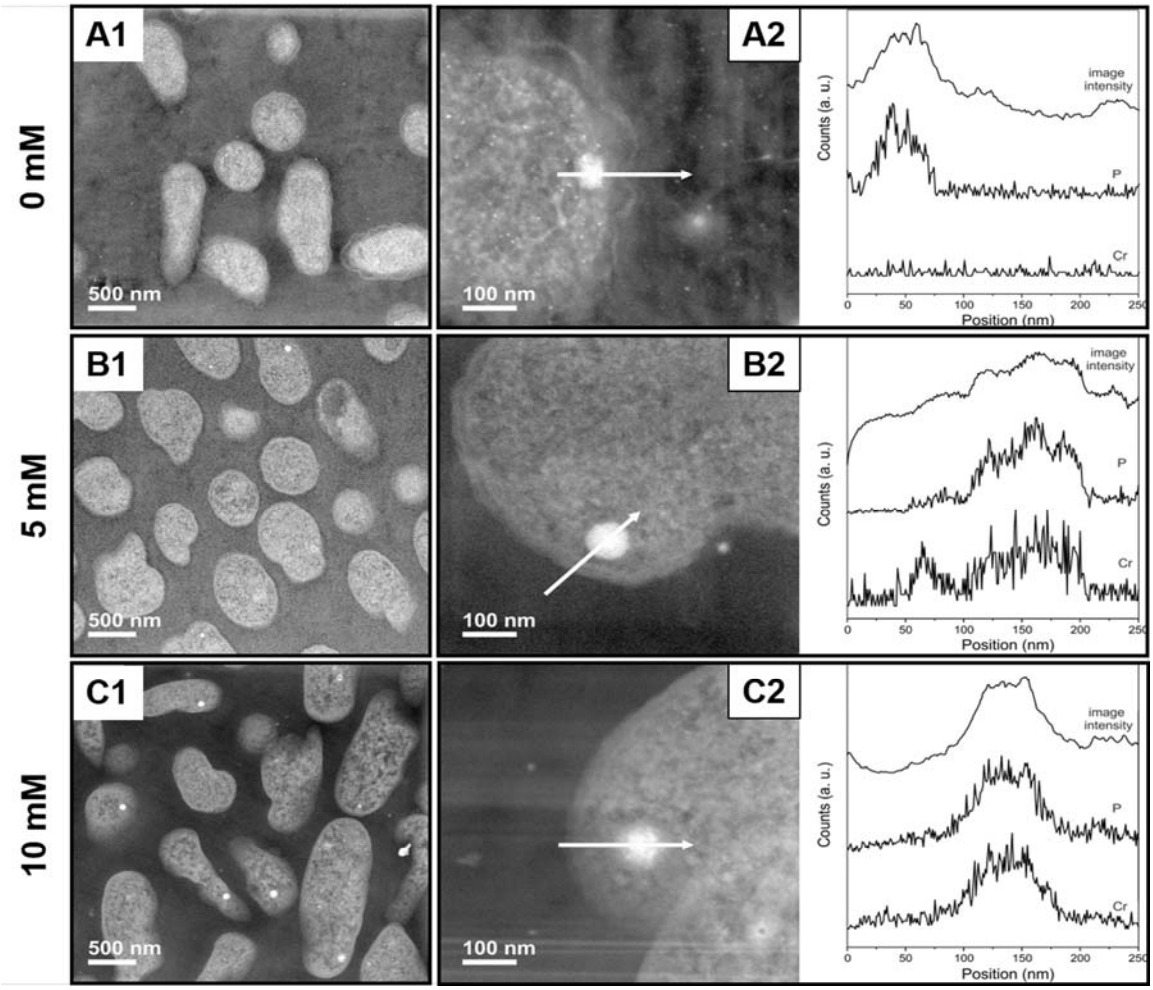
0 mM
5 mM
10 mM
A1
A2
B1
B2
C1
C2
500 nm
100 nm
image intensity
P
Cr
Counts (a. u.)
Position (nm)
0
50
100
150
200
250